J|A|C|S
ARTICLES
Published on Web 08/01/2006

Color Tuning in Rhodopsins: The Mechanism for the Spectral Shift between Bacteriorhodopsin and Sensory Rhodopsin II

Michael Hoffmann,[†] Marius Wanko,[†] Paul Strodel,[‡] Peter H. König,[†] Thomas Frauenheim,[†] Klaus Schulten,[§] Walter Thiel,[||] Emad Tajkhorshid,*[,§] and Marcus Elstner*[,†,‡]

Contribution from the Theoretische Physik, Universität Paderborn, Warburger Str. 100, 33098 Paderborn, Germany, Molekulare Biophysik, Deutsches Krebsforschungszentrum, 69120 Heidelberg, Germany, Beckmann Institute, University of Illinois at Urbana-Champaign, 405 North Mathews, Urbana, Illinois 61801, and MPI für Kohlenforschung, 45470 Mülheim an der Ruhr, Germany

Received March 27, 2006; E-mail: elstner@phys.uni-paderborn.de; emad@ks.uiuc.edu

Abstract: The mechanism of color tuning in the rhodopsin family of proteins has been studied by comparing the optical properties of the light-driven proton pump bacteriorhodopsin (bR) and the light detector sensory rhodopsin II (sRII). Despite a high structural similarity, the maximal absorption is blue-shifted from 568 nm in bR to 497 nm in sRII. The molecular mechanism of this shift is still a matter of debate, and its clarification sheds light onto the general mechanisms of color tuning in retinal proteins. The calculations employ a combined quantum mechanical/molecular mechanical (QM/MM) technique, using a DFT-based method for ground state properties and the semiempirical OM2/MRCI method and ab initio SORCI method for excited state calculations. The high efficiency of the methodology has allowed us to study a wide variety of aspects including dynamical effects. The absorption shift as well as various mutation experiments and vibrational properties have been successfully reproduced. Our results indicate that several sources contribute to the spectral shift between bR and sRII. The main factors are the counterion region at the extracellular side of retinal and the amino acid composition of the binding pocket. Our analysis allows a distinction and identification of the different effects in detail and leads to a clear picture of the mechanism of color tuning, which is in good agreement with available experimental data.

I. Introduction

Retinal proteins, also known as rhodopsins, play important roles in the processes of vision, bioenergetics, and phototaxis.[1,2] The crucial light-absorbing chromophore, a retinal bound via a protonated Schiff base linkage to the apoprotein, triggers the response of the protein to light. The protein environment drastically modulates the absorption maximum of the chromophore from a value of about 440 nm in organic solvents[3] to values ranging from 425 to 560 nm in light sensitive cone pigments[4] responsible for color vision. The mechanism by which protein environments regulate the absorption maximum of the chromophore (spectral tuning) is therefore of fundamental importance for understanding the process of color vision.

The cellular membrane of Halobacteria contains four different photoactive rhodopsins: bacteriorhodopsin (bR),[5−7] halorhodopsin (hR),[8] sensory rhodopsin I (sRI),[9] and sensory rhodopsin II (sRII),[10,11] also called phoborhodopsin (ppR). These proteins share the same basic structure of seven trans-membrane helices enclosing a chromophore binding site containing an all-trans retinal. Upon absorption of light, the chromophore isomerizes into a 13-cis conformation which induces either light-driven ion transport (proton transfer from the cytoplasmic to the extracellular side of the cell membrane in the case of bR[7,12] or chloride transport in hR[8]) or photosensory signaling (in sRI and sRII[11,13]).

With regard to the absorption maximum (λ_{max}), ppR is significantly different from bR, hR, and sRI: the absorption maximum of ppR (497 nm)[14] is blue shifted by about 70 nm relative to the others, which absorb in the range of 560−590 nm. This is very remarkable since halobacterial rhodopsins share

[†] Universität Paderborn.
[‡] Deutsches Krebsforschungszentrum.
[§] University of Illinois at Urbana-Champaign.
[||] MPI für Kohlenforschung.

(1) Spudich, J. L.; Yang, C.; Jung, K.; Spudich, E. N. *Annu. Rev. Cell Dev. Biol.* **2000**, *16*, 365.
(2) van der Horst, M. A.; Hellingwerf, K. J. *Acc. Chem. Res.* **2004**, *37*, 13.
(3) Logunov, S. L.; Song, L.; El-Sayed, M. A. *J. Phys. Chem.* **1996**, *100*, 18586−18591.
(4) Kochendoerfer, G. G.; Lin, S. W.; Sakmar, T. T.; Mathies, R. A. *TIBS* **1999**, *24*, 300−305.
(5) Haupts, U.; Tittor, J.; Oesterhelt, D. *Annu. Rev. Biophys. Biomol. Struct.* **1999**, *28*, 367.
(6) Lanyi, J. *J. Phys. Chem. B* **2000**, *104*, 11441.
(7) Lanyi, J. *Annu. Rev. Physiol.* **2004**, *66*, 144−167.
(8) Lanyi, J. K. *Annu. Rev. Biophys. Biophys. Chem.* **1986**, *15*, 11.
(9) Hoff, W. D.; Jung, K.; Spudich, J. L. *Annu. Rev. Biophys. Biomol. Struct.* **1997**, *26*, 223.
(10) Sasaki, J.; Spudich, J. L. *Biochim. Biophys. Acta* **2000**, *1460*, 230.
(11) Spudich, J. L.; Bogomolni, R. A. *Annu. Rev. Biophys. Biophys. Chem.* **1988**, *17*, 193.
(12) Neutze, R.; Pebay-Peyroula, E.; Edmann, E.; Royant, A.; Navarro, J.; Landau, E. *Biochim. Biophys. Acta* **2002**, *1565*, 144−167.
(13) Spudich, J. L.; Bogomolni, R. A. *Nature (London)* **1984**, *312*, 509.
(14) Chizhov, I.; Schmies, G.; Seidel, R.; Sydor, J. R.; Lüttenberg, B.; Engelhard, M. *Biophys. J.* **1998**, *75*, 999.

10.1021/ja062082i CCC: $33.50

the same chromophore and are highly homologous in their structure, raising the question as to how the absorption maximum is regulated in bR, hR, sRI, and ppR.

In bR and ppR, the amino acid compositions of the binding pocket differ only in 10 amino acids within 5 Å of the chromophore so that the observed large difference in λ_{max} is unexpected. Because of this ostensible conflict, the spectral shift has been studied extensively with experimental[15−19] as well as theoretical methods.[20,21]

Several mechanisms for color tuning in these systems have been proposed:[22] (i) coplanarization of the ring−chain system and further distortion of the chromophore structure;[23−27] (ii) electrostatic interaction of the chromophore with ionic, polar and polarizable groups of the protein environment;[28−31] and (iii) a change in the interactions between the chromophore and its complex counterion.[32−34]

The crystal structures of bR[35] and ppR[36,37] show differences in the retinal geometry. However, FTIR spectroscopy[38] and previous theoretical calculations[20,21] agree that mechanism (i) appears to be of minor importance in the case of bR vs ppR. Hence, the changes in chromophore geometry cannot explain the spectral shift between bR and ppR.

Mutation experiments have elucidated the role of mechanism (ii) in the color tuning by identifying residues in the retinal binding pocket which are involved in the spectral shift.[15−19,39−42] In particular, Shimono and co-workers[15−19] have extensively studied the differences between bR and ppR. Single mutation of residues in the binding pocket of ppR[15,16] showed that each side chain has only small contributions to the color tuning. Even simultaneous mutation of multiple side chains could only produce parts of the spectral shift.[15,16] A prominent example is the ppR mutant 'bR/ppR' with a binding pocket identical to that of bR, i.e., all 10 different residues within 5 Å of the chromophore were replaced by the corresponding ones in bR. For this multiple mutant, about 40% of the shift was obtained.

These results indicate that mechanism (ii) is insufficient to explain the total spectral shift if only a single or a small number of residues are considered.

Mechanism (iii), the change in the interactions between the chromophore and its complex counterion or hydrogen-bond acceptor, has also found to be of importance. On the basis of frequency shifts of the Schiff base vibrations, Kandori and co-workers[17,38,43] found that the hydrogen bond between the protonated Schiff base and the counterion complex is stronger in ppR than in bR. Interestingly, FTIR measurements on the bR/ppR mutant indicated that the strength of the counterion interaction is the same as in ppR, although the binding pocket is identical to that of bR. This result shows that the mechanisms (ii) and (iii) are indeed working independently. Thus, the bR/ppR mutant provides the opportunity to distinguish between the contributions of mechanisms (ii) and (iii). Furthermore, two of the counterion residues (the aspartic acids) and three water molecules form a pentagonal cluster structure, a hydrogen bonded network, in the following abbreviated HBN. This pentagonal structure was proposed to be distorted in ppR in contrast to bR, which was later confirmed by crystal structures.[35−37] So the question arises, whether and how these observations are related to the λ_{max} difference.

In recent work by Shimono et al.,[18] the distorted hydrogen bonded cluster was attributed to the different position of the guanidinium group of arginine 72 (Arg72) in ppR—it points toward the extracellular side in ppR forming a salt bridge with aspartate 193 (Asp193), while the corresponding residue in bR, Arg82, points toward the cytoplasmic side and thus interacts more strongly with the HBN. The importance of Arg72 was also pointed out by Luecke et al.[37] in their work about X-ray structures of ppR.

Ren et al.[20] came to a similar conclusion about the importance of Arg72 in their theoretical work based on the X-ray structures and quantum mechanical calculations for active site models. The different positions of the guanidinium group of Arg82/72 (bR/ppR) were suggested to be the main reason for the spectral shift because they influence the charge distribution on the counterion residues differently in bR and ppR.

The combined QM/MM calculations of Hayashi et al.,[21] in contrast, suggested that the spectral shift is induced by a shift of helix G that results in a shorter Schiff base-counterion residue (Asp201) distance in ppR, and hence a stronger chromophore-counterion interaction. However, this shorter distance is not apparent in the underlying crystal structure.[36]

So the theoretical studies came to different conclusions about the principal mechanism of spectral tuning—different positions

(15) Shimono, K.; Kitami, M.; Iwamoto, M.; Kamo, N. *Biophys. Chem.* **2000**, *87*, 225.
(16) Shimono, K.; Iwamoto, M.; Sumi, M.; Kamo, N. *Biochim. Biophys. Acta* **2001**, *1515*, 92.
(17) Shimono, K.; Furutani, Y.; Kandori, H.; Kamo, N. *Biochemistry* **2002**, *41*, 6504−6509.
(18) Shimono, K.; Hayashi, T.; Ikeura, Y.; Sudo, Y.; Iwamoto, M.; Kamo, N. *J. Biol. Chem.* **2003**, *278*, 23882.
(19) Shimono, K.; Iwamoto, M.; Sumi, M.; Kamo, N. *Photochem. Photobiol.* **2000**, *72*, 141.
(20) Ren, L.; Martin, C. H.; Wise, K. J.; Gillespie, N. B.; Luecke, H.; Lanyi, J. K.; Spudich, J. L.; Birge, R. R. *Biochemistry* **2001**, *40*, 13906−13914.
(21) Hayashi, S.; Tajkhorshid, E.; Pebay-Peyroula, E.; Royant, A.; Landau, E. M.; J.; N.; Schulten, K. *J. Phys. Chem. B* **2001**, *105*, 10124−10131.
(22) Nakanishi, K.; Balogh-Nair, Y.; Arnaboldi, M.; Tsujimoto, K.; Honig, B. *J. Am. Chem. Soc.* **1980**, *102*, 7945.
(23) Van der Steen, R.; Biesheuvel, B. L.; Lugtenburg, J. *J. Am. Chem. Soc.* **1986**, *108*, 6410.
(24) Harbison, G. S.; Mulder, P. P. J.; Pardoen, J. A. *Biochemistry* **1985**, *24*, 6955.
(25) Harbison, G. S.; Mulder, P. P. J.; Pardoen, J. A. *J. Am. Chem. Soc.* **1985**, *107*, 4810.
(26) Wada, M.; Sakutai, M.; Inoue, Y.; Tamura, Y.; Watanabe, Y. *J. Am. Chem. Soc.* **1994**, *116*, 1537.
(27) Kakitani, H.; Kakitani, T.; Rodman, H.; Honig, B. *Photochem. Photobiol.* **1985**, *41*, 471.
(28) Kochendoerfer, G.; Wang, Z.; Oprian, D. D.; Mathies, R. A. *Biochemistry* **1997**, *36*, 6577−6587.
(29) Irving, C. S.; Byers, G. W.; Leermake, P. A. *J. Am. Chem. Soc.* **1969**, *91*, 2141.
(30) Irving, C. S.; Byers, G. W.; Leermake, P. A. *Biochemistry* **1970**, *9*, 858.
(31) Beppu, Y.; Kakitani, T. *Photochem. Photobiol.* **1994**, *59*, 660.
(32) Birge, R. R.; Murray, L. M.; Pierce, B. M.; Akita, H.; Balogh-Nair, V.; Findsen, L. A.; Nakanishi, K. *Proc. Natl. Acad. Sci., U.S.A.* **1985**, *82*, 4117−4121.
(33) Baasov, T.; Friedman, N.; Sheves, M. *Biochemistry* **1987**, *26*, 3210−3217.
(34) Hu, J.; Griffin, R. G.; Herzfeld, J. *Proc. Natl. Acad. Sci. U.S.A.* **1994**, *91*, 8880−8884.
(35) Lücke, H.; Schobert, B.; Richter, H. T.; Cartailler, J. P.; Lanyi, J. K. *J. Mol. Biol.* **1999**, *291*, 899−911.
(36) Royant, A.; Nollert, P.; Edmann, K.; Neutze, R.; Landau, E. M.; Pebay-Peyroula, E.; Navarro, J. *Proc. Natl. Acad. Sci., U.S.A.* **2001**, *98*, 10131−10136.
(37) Luecke, H.; Schobert, B.; Lanyi, J.; Spudich, E. N.; Spudich, J. L. *Science* **2001**, *293*, 1499−1503.
(38) Kandori, H.; Shimono, K.; Sudo, Y.; Iwamoto, M.; Shichida, Y.; Kamo, N. *Biochemistry* **2001**, *40*, 9238−9246.
(39) Greenhalgh, D. A.; Farrens, D. L.; Subramaniam, S.; Khorana, H. G. *J. Biol. Chem.* **1993**, *268*, 20305.
(40) Mogi, T.; Marti, T.; Khorana, H. G. *J. Biol. Chem.* **1989**, *264*, 14197.
(41) Hackett, N. R.; Stern, L. J.; Chao, B. H.; Kronis, K. A.; Khorana, H. G. *J. Biol. Chem.* **1987**, *262*, 9277.
(42) Ahl, P. L.; Stern, L. J.; Düring, D.; Mogi, T.; Khorana, H. G.; Rothschild, K. J. *J. Biol. Chem.* **1988**, *263*, 13594.
(43) Shimono, K.; Furutani, Y.; Kamo, N.; Kandori, H. *Biochemistry* **2003**, *42*, 7801−7806.

of the guanidinium group of Arg82/72 or a shorter Schiff base-counterion (Asp201) distance in ppR. Both theoretical studies concluded that a major contribution to the spectral shift is due to geometrical differences of a particular amino acid in bR and ppR. This is important because it provides an explanation for the failure of mutational studies of the retinal binding pocket to completely reverse the spectral shift. However, the contributions from other amino acids of the binding pocket, which are experimentally known to account for approximately 40% of the shift,[16] were not taken into account in these studies.

Because of the open issues presented above, we revisit the problem of color regulation in bR vs ppR with focus on reproducing and interpreting the available experimental data. In this work, we calculate excitation energies after QM/MM optimization and along MD trajectories. Further, we study the effect of the chromophore structure, the counterion residues, and the hydrogen bonded network. By calculating the effects of mutations, we will interpret experimental observations and study the influence of individual residues. A perturbation analysis will reveal the effect of every residue in both proteins. The calculated vibrational frequencies offer further connection to experimental data and elucidate the strength of the hydrogen bonds in both proteins and the mutant bR/ppR.

II. Methods

The general computational strategy employed in this work is the result of an extensive assessment of various methodologies with regard to their performance in the description of the retinal chromophore, its ground-state geometry, optical properties, and response to electrostatic and steric interactions with its environment.[44] The overall approach is based on ground-state geometry optimization and MD simulations in a combined QM/MM framework[45] using the approximate density functional method SCC-DFTB[46] for the QM region and the CHARMM27 force field[47] for the remainder of the protein.

SCC-DFTB[46] has been applied in several QM/MM MD studies before.[48−55] With an efficiency comparable to semiempirical methods such as MNDO, AM1, or PM3, SCC-DFTB allows for long-time scale MD or MC simulations, which are not feasible at the ab initio or DFT level of theory. SCC-DFTB has been shown to describe ground-state properties of the protonated Schiff base (bond length alternation of the polyene chain, torsional barriers etc.) with an accuracy comparable to full DFT methods.[56] In particular, with respect to the bond length alternation (BLA), which plays an important role in the spectral tuning, SCC-DFTB structures are in good agreement with B3LYP, MP2, and CASPT2 calculations.[44,57−59]

The calculation of excitation energies and excited-state properties for the QM/MM structures is carried out using MRCI methods on the semiempirical (OM2/MRCI) and ab initio (SORCI) level of theory. The electrostatic potential of the MM region, as represented by fixed point charges of the CHARMM force field, is included in the corresponding QM Hamiltonians.

The quantitative calculation of excitation energies of retinal proteins is challenging and it has been shown that multireference approaches[99] are required to reliably predict spectral shifts.[44] We employed the ab initio method SORCI as highest computational level that is applicable to the full chromophore and few additional amino acid side chains and the semiempirical OM2/MRCI for conformational sampling of the excitation energy.

The *Spectroscopy ORiented Configuration Interaction* (SORCI) method[60] is part of the ORCA quantum chemical package.[61] SORCI combines the concepts of classical multireference CI and multireference perturbation theory by dividing the first-order interacting space into weakly and strongly perturbing configurations. While the latter are treated variationally, the contributions of the former are included by second-order Møller−Plesset perturbation theory. The use of approximate natural orbitals eliminates the problem of choosing a suitable

(44) Wanko, M.; Hoffmann, M.; Strodel, P.; Koslowski, A.; Thiel, W.; Neese, F.; Frauenheim, T.; Elstner, M. *J. Phys. Chem. B* **2005**, *109*, 3606−3615.
(45) Cui, Q.; Elstner, M.; Kaxiras, E.; Frauenheim, T.; Karplus, M. *J. Phys. Chem. B* **2001**, *105*, 569.
(46) Elstner, M.; Porezag, D.; Jungnickel, G.; Elsner, J.; Haugk, M.; Frauenheim, T.; Suhai, S.; Seifert, G. *Phys. Rev. B* **1998**, *58*, 7260−7268.
(47) MacKerell, A. D. et al. *J. Phys. Chem. B* **1998**, *102*, 3586.
(48) Elstner, M.; Frauenheim, T.; Suhai, S. *J. Mol. Struct.* **2003**, *632*, 29−41.
(49) Elstner, M.; Cui, Q.; Munih, P.; Kaxiras, E.; Frauenheim, T.; Karplus, M. *J. Comput. Chem.* **2003**, *24*, 565.
(50) Zhang, X.; Harrison, D. H. T.; Cui, Q. *J. Am. Chem. Soc.* **2002**, *124*, 14871.
(51) Formaneck, M. S.; Li, G.; Zhang, X.; Cui, Q. *J. Theor. Comput. Chem.* **2002**, *1*, 53.
(52) Cui, Q.; Elstner, M.; Karplus, M. *J. Phys. Chem. B* **2002**, *106*, 2721.
(53) Li, G.; Cui, Q. *J. Am. Chem. Soc.* **2003**, *125*, 15028.
(54) Li, G.; Zhang, X.; Cui, Q. *J. Phys. Chem. B* **2003**, *107*, 8643.
(55) König, P. H.; Ghosh, N.; Hoffmann, M.; Elstner, M.; Tajkhorshid, E.; Frauenheim, T.; Cui, Q. *J. Phys. Chem. A* **2006**, *110*, 548.
(56) Zhou, H.; Tajkhorshid, E.; Frauenheim, T.; Suhai, S.; Elstner, M. *Chem. Phys.* **2002**, *277*, 91−103.
(57) Fantacci, S.; Migani, A.; Olivucci, M. *J. Phys. Chem. A* **2004**, *108*, 1208−1213.
(58) Page, C. S.; Olivucci, M. *J. Comput. Chem.* **2003**, *24*, 298−309.
(59) Lee, H. M.; Kim, J.; Kim, J. C.; Kim, K. S. *J. Chem. Phys.* **2002**, *116*, 6549−6559.
(60) Neese, F. *J. Chem. Phys.* **2003**, *119*, 9428.
(61) Neese, F. "ORCA − An ab initio, density functional and semiempirical program package, Version 2.3 − Revision 09, February 2004", Max Planck Institut für Strahlenchemie, Mülheim., 2004.
(62) Schaefer, A.; Horn, H.; Ahlrichs, R. *J. Chem. Phys.* **1992**, *97*, 2571.
(63) Weber, W. *Ein neues semiempirisches NDDO−Verfahren mit Orthogonalisierungskorrekturen.*, Thesis, Universität Zürich, 1996.
(64) Weber, W.; Thiel, W. *Theor. Chem. Acc.* **2000**, *103*, 495−506.
(65) Koslowski, A.; Beck, M. E.; Thiel, W. *J. Comput. Chem.* **2003**, *24*, 714−726.
(66) Strodel, P.; Tavan, P. *J. Chem. Phys.* **2002**, *117*, 4677.
(67) Sasaki, J.; Lany, J. K.; Needleman, R.; Yoshizawa, T.; Maeda, A. *Biochemistry* **1994**, *33*, 3178.
(68) Brown, L. S.; Sasaki, J.; Kandori, H.; Maeda, A.; Needleman, R.; Lanyi, J. K. *J. Biol. Chem.* **1995**, *270*, 27122−27126.
(69) Brooks, B. R.; Bruccoleri, R. E.; Olafson, B. E.; States, D. J.; Swaminathan, S.; Karplus, M. *J. Comput. Chem.* **1983**, *4*, 187.
(70) Dinner, A. R.; Lopez, X.; Karplus, M. *Theor. Chem. Acc.* **2003**, *109*, 118.
(71) Simonson, T.; Archontis, G.; Karplus, M. *J. Phys. Chem. B* **1997**, *101*, 8349.
(72) König, P.; Hoffmann, M.; Frauenheim, T.; Cui, Q. *J. Phys. Chem. B* **2005**, *109*, 9082.
(73) Nose, S. *J. Chem. Phys.* **1984**, *81*, 551.
(74) Hoover, W. *Phys. Rev. A* **1985**, *31*, 1695.
(75) Warshel, A.; Chu, Z. T. *J. Phys. Chem. B* **2001**, *105*, 9857−9871.
(76) Nonella, M.; Mathias, G.; Tavan, P. *J. Phys. Chem. A* **2003**, *107*, 8638.
(77) Belrhali, H.; Nollert, P.; Royant, A.; Menzel, C.; Rosenbusch, J.; Landau, E.; Pebay-Peyroula, E. *Structure* **1999**, *7*, 909.
(78) Luecke, H.; Richter, H. T.; Lanyi, J. K. *Science* **1998**, *280*, 1934.
(79) Vreven, T.; Morokuma, K. *Theor. Chem. Acc.* **2003**, *109*, 125−132.
(80) Hayashi, S.; Ohmine, I. *J. Phys. Chem. B* **2000**, *104*, 10678−10691.
(81) Kandori, H.; Furutani, Y.; Shimono, K.; Shichida, Y.; Kamo, N. *Biochemistry* **2001**, *40*, 15693−15698.
(82) Birge, R. R.; Zhang, C. *J. Chem. Phys.* **1990**, *92*, 7178.
(83) Houjou, H.; Inoue, Y.; Sakurai, M. *J. Phys. Chem. B* **2001**, *105*, 867−879.
(84) Mathies, R.; Stryer, L. *Proc. Natl. Acad. Sci., U.S.A.* **1976**, *73*, 2169.
(85) González-Luque, R.; Garavelli, M.; Bernardi, F.; Merchán, M.; Robb, M. A.; Olivucci, M. *Proc. Natl. Acad. Sci., U.S.A.* **2000**, *97*, 9379.
(86) Cembran, A.; Bernardi, F.; Olivucci, M.; Garavelli, M. *J. Am. Chem. Soc.* **2003**, *125*, 12509.
(87) Hufen, J.; Sugihara, M.; Buss, V. *J. Phys. Chem.* **2004**, *108*, 20419.
(88) Ferre, N.; Olivucci, M. *J. Am. Chem. Soc.* **2003**, *125*, 6868.
(89) Riesle, J.; Oesterheld, D.; Dechner, N. A.; Heberle, J. *Biochemistry* **1996**, *35*, 6635.
(90) Hayashi, S.; Tajkhorshid, E.; Kandori, H.; Schulten, K. *J. Am. Chem. Soc.* **2004**, *126*, 10516.
(91) Kochendoerfer, G.; Lin, S. W.; Sakmar, T. P.; Mathies, R. A. *Trends Biochem. Sci.* **1999**, *24*, 300.
(92) Baasov, T.; Sheves, M. *J. Am. Chem. Soc.* **1985**, *107*, 7524.
(93) Lin, S.; Imamoto, Y.; Fukada, Y.; Shichida, Y.; Yoshizawa, T.; Mathies, R. *Biochemistry* **1994**, *33*, 2151.
(94) Heyde, M. E.; Gill, D.; Kilponen, R. G.; Rimai, L. *J. Am. Chem. Soc.* **1979**, *93*, 6776.
(95) Birge, R. R. *Biochim. Biophys. Acta* **1990**, *1016*, 293.
(96) Zhang, Y.; Kua, J.; McCammon, J. A. *J. Phys. Chem. B* **2003**, *107*, 4459.
(97) Lin, S. W.; Groesbeek, M.; van der Hoef, I.; Verdegem, P.; Lugtenburg, J.; Mathies, R. A. *J. Phys. Chem. B* **1998**, *102*, 2787.
(98) Schreiber, M.; Buss, V.; Sugihara, M. *J. Chem. Phys.* **2003**, *119*, 12045−12048.
(99) The use of local exchange functionals in TDDFT as well as an unbalanced inclusion of dynamic and static correlation in methods like CASSCF or CIS are problematic in this context.

single-particle basis whose quality would affect the final CI result. SORCI gains computational efficiency by use of several thresholds which have been carefully adjusted for applications to the systems under study.[100] The employed basis set is Ahlrichs SV(P),[62] which is appropriate for calculations on the full chromophore.

The semiempirical OM2 Hamiltonian[63,64] has been chosen for MRCI calculations[65] because for extended CI treatments this method is expected to be superior to traditional semiempirical Hamiltonians like MNDO or AM1, which underestimate the HOMO−LUMO gap due to their neglect of nonorthogonality between the atomic basis functions.[64] By applying orthogonalization corrections to the Fock matrix, OM2 overcomes this problem and thus yields improved MRCI excitation energies (as has been shown in[66] for the case of butadiene) without any reparametrization. We have shown earlier[44] that OM2/MRCI reproduces excited-state properties of retinal chromophores in agreement with CASPT2 and SORCI calculations. Although absolute excitation energies are systematically overestimated, OM2/MRCI is able to predict spectral shifts due to changes in the electrostatic environment, as caused by mutations, or conformational changes during MD runs with great reliability. The OM2/MRCISD calculations in this work were performed with version 6.1 of the MNDO99 program using an active orbital window of 15 occupied and 15 virtual orbitals that are selected from a preliminary CI run. No individual configuration selection was applied.

The coordinates of bR and ppR were obtained from the X-ray crystallographic structures of Luecke et al.[35] (PDB code 1C3W) and Royant et al.[36] (PDB code 1H68), respectively. For bR, standard protonation states were assumed except for Asp96, Asp115, and Glu204, which were modeled in their protonated form.[67,68] In ppR, all titratable residues were assumed to be charged.[21] Hydrogen atoms were added using the HBUILD module of the CHARMM program package.[69] The systems contain 3694 atoms and 23 crystal water for bR and 3495 atoms and 27 crystal water for ppR.

During geometry optimizations and molecular dynamics (MD) simulations, C_α-atoms with a distance to the Schiff base greater than 14 Å were harmonically restrained to their initial positions. All atoms were optimized or propagated during geometry optimizations and MD simulations.

To mimic the screening effect of bulk solvent, a Poisson−Boltzmann (PB) charge scaling scheme was used as proposed by Dinner et al.[70] The method scales down the partial charges for charged residues exposed to the solvent on the surface of the protein according to a set of PB calculations.[71]

The QM segment comprises retinal (63 atoms, charge +1), the boundary between the QM and MM region was chosen at the $C_\alpha-C_\beta$ bond and link atoms were introduced to saturate the valence of the QM boundary atoms. The interactions at the boundary are treated using the divided frontier charge scheme recently proposed and tested by Koenig et al.[72] For the electrostatic description of the MM part, electrostatic force shifting with a cutoff of 13.0 Å was used.

The QM/MM dynamics simulations employed constant-temperature MD defined by the Nose−Hoover equations[73,74] of motion, with a time step of 1.0 fs and a temperature of 300 K. In total 1.8 ns, split into three independent simulations that started from different random seeds, were performed for both proteins. For each simulation an equilibration run of 100 ps was followed by a 500 ps production run.

On the basis of the trajectories, the absorption spectra were obtained by calculating the excitation energies with OM2/MRCI along the trajectories[75] and using the corresponding histograms as an approximation to the absorption spectra. For each histogram 1000 excitation energies with a time interval of 0.1 ps were collected and a bin width of 0.05 eV was used. The structures were obtained from the last 100 ps of one of the simulations for bR and ppR, respectively. The vibrational properties were calculated using the autocorrelation function of the velocity obtained from QM/MM dynamics.[76]

(100) The thresholds used in this work are as follows: $T_{Pre} = 10^{-3}$, $T_{Nat} = 10^{-6}$, and $T_{Sel} = 10^{-6}E_h$ (see Supporting Information of ref 44). Only core orbitals were frozen.

III. Results

In the following, we present the results of our calculations on the spectral shift between bR and ppR. In section IIIA and IIIB, we explore the spectral shift based on QM/MM minimized structures. In section IIIC, a perturbation analysis is used to investigate the influence of each residue of the protein on the excitation energy. In section III D, we address the impact of residues in the binding pocket in more detail using mutation experiments. A vibrational analysis in section III E and the calculation of the spectral shift on the basis of QM/MM dynamical simulations in section III F finalize this study.

A. Comparison of Structures. Geometry optimization of the X-ray structures of bR and ppR (PDB codes: 1C3W and 1H68) using the SCC-DFTB/CHARMM scheme yields nearly identical geometries for the chromophore. Previous theoretical studies[20,21] came to similar results, while the crystal structures[37,77,78] show larger deviations between bR and ppR in the lysine side chain to which the retinal is covalently bound (see Hayashi et al.[21] for more details). Despite the similarity of the chromophore structures, the bond length alternation (BLA) of retinal, calculated as the difference between the average single and double bond lengths along the polyene chain, is clearly different for the QM/MM optimized structures of bR (0.056 Å) and ppR (0.065 Å).[101]

Further, the distance between the β-ionone ring and the C_ζ atom of Arg82/72 is different in bR and ppR due to the different orientation of the guanidinium group in bR and ppR (Figure 1). A detailed structural comparison of the complex consisting of the counterion residues and the three water molecules in the retinal binding pocket (which together are referred to as extended HBN in the following text) is summarized in Table 1.

Experimental studies[81] emphasized a structural difference in the HBN for bR and ppR (Figure 1). Comparing the X-ray structures of the HBN, the ppR (1H68) structure shows a 'distortion' (with respect to bR) as indicated by a larger W401−W406/W401−W400 distance, a larger distance between C_ζ of Arg82/72 and the Schiff base, and a shorter distance of the Schiff base nitrogen to the oxygen of W402 in ppR. These differences are not as pronounced in our QM/MM optimized structures. The deviation of our structures from the underlying crystal structures is within the margin of fluctuations between the available experimental structures (see Table 1).

Theoretical studies by Hayashi et al.[80] and Vreven et al.[79] yielded QM/MM optimized structures for bR that differ from ours and the crystal structures regarding the HBN in one respect:[102] the water molecule W402 is hydrogen bonded to the $O_{\delta1}$ atom of Asp212, rather than the $O_{\delta2}$ atom (see Figure 1 for notation) as in our and the crystal structures (1BRX, 1C3W) (Table 1).[103] As a consequence, the distances between the oxygen of W402 to $O_{\delta1}$ and $O_{\delta2}$ differ significantly (e.g., 2.82 and 4.07 Å in ref 80), while this difference is much smaller in

(101) This value has a direct relationship to the excitation energy, as discussed in detail later.

(102) Other geometrical variations are in the order of 0.3 Å and of minor importance. They may be due to differences in the applied quantum mechanical potentials or to local minima found by different optimization techniques. As will be discussed below (sec. III F), these variables show fluctuations of similar magnitude along MD trajectories.

(103) This deviation from the crystal structures was already pointed out in ref 80.

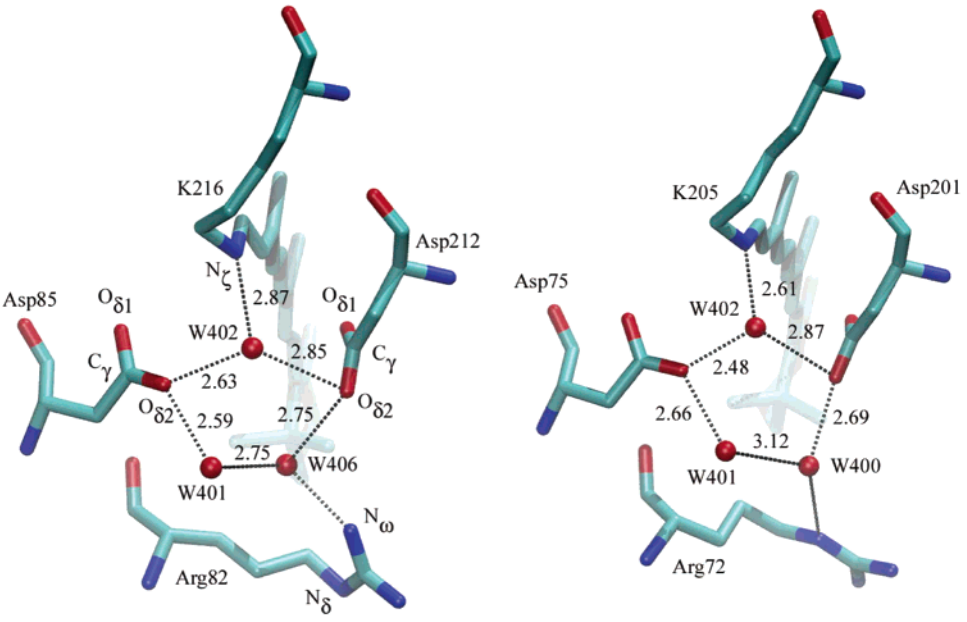

Figure 1. Hydrogen bonded network of bR (1C3W, left) and ppR (1H68). (Distances in Å).

Table 1. Selected Geometrical Parameters of the Retinal Binding Site for QM/MM Optimized Structures of This Study, X-ray Structures, and from Previous Theoretical Studies[a]

		present work		*x*-ray structures					previous works	
		bR	ppR	1C3W (bR)	1BRX (bR)	1QHJ (bR)	1H68 (ppR)	1JGJ (bR)	Vreven[b] (bR)	Hayashi[c] (bR)
$RET_{N\zeta}$	O(W402/402)	2.81	2.82	2.87	2.68	2.85	2.61	2.64	2.80	2.63
O(W402/402)	$O_{\xi 2}$(Asp85/75)	2.57	2.59	2.63	2.80	2.57	2.48	2.40	2.55	2.58
O(W402/402)	$O_{\xi 2}$(Asp212/201)	2.75	2.71	2.85	3.36	3.17	2.87	3.06	4.11	4.07
$RET_{N\zeta}$	$O_{\xi 1}$(Asp85/75)	3.66	3.67	3.79	4.29	3.65	4.07	4.15	3.59	
$RET_{N\zeta}$	$O_{\xi 2}$(Asp85/75)	4.33	4.36	4.38	4.19	4.17	4.28	3.98	3.91	
$RET_{N\zeta}$	C_{γ}(Asp85/75)	4.35	4.41	4.45	4.66	4.28	4.58	4.42		
$RET_{N\zeta}$	$O_{\xi 1}$(Asp212/201)	4.02	4.28	3.74	3.66	3.96	4.05	3.82	3.77	
$RET_{N\zeta}$	$O_{\xi 2}$(Asp212/201)	4.77	4.71	4.85	4.87	5.18	4.63	4.89		
$RET_{N\zeta}$	C_{γ}(Asp212/201)	4.29	4.36	4.12	3.99	4.41	4.11	4.25		5.2[d]
O(W402/402)	$O_{\xi 1}$(Asp85/75)	3.56	3.55	3.65	4.20	3.71	3.67	3.93		
O(W402/402)	$O_{\xi 1}$(Asp212/201)	3.48	3.71	3.26	3.55	3.32	3.65	3.35	2.59	2.82
O(W401/401)	$O_{\xi 2}$(Asp85/75)	2.60	2.59	2.59	2.57	2.81	2.66	2.72	2.62	2.63
O(W401/401)	O(W406/400)	2.74	2.73	2.75		3.01	3.13	3.19	2.67	2.77
O(W406/400)	$O_{\xi 2}$(Asp212/212)	2.61	2.65	2.75		2.63	2.69	2.50	2.58	2.78
O(W406/400)	$N_{\omega/\delta}$(Arg82/72)	2.77	2.89	2.49		2.58	3.03	3.74		2.72
$RET_{N\zeta}$	C_{ζ}(Arg82/72)	10.32	10.15	9.39	8.46	9.71	10.14	10.45		
RET_{C6}	C_{ζ}(Arg82/72)	11.59	10.91	11.6	10.99	11.60	10.92	11.10		

[a] Distances in Å; the two residue numbers specified refer to bR and ppR, respectively. [b] Ref 79. [c] Refs 21, 80. [d] Value taken from ref 21.

our QM/MM optimized structures (Table 1). Moreover, the distance between the Schiff base nitrogen and C_{γ} of Asp212 is increased from 4.12 Å (1C3W) to 5.2 Å in Hayashi's structure.[21] This was proposed to be responsible for the difference in excitation energy between ppR and bR, since the corresponding distance in ppR is clearly shorter (4.5 Å). In our QM/MM optimized structures of bR and ppR, this distance is similar in both cases (4.29 Å in bR, 4.36 Å in ppR), in good agreement with the values found in the various X-ray structures.

In the theoretical study by Ren et al.,[20] the geometry of the chromophore and the positions of the hydrogens were optimized while the positions of all other atoms were held fixed during the optimization. For the optimized chromophore a similar structure was found in bR and ppR. Other geometrical parameters like the structure of the HBN (and, e.g., the orientation of the guanidinium group of Arg72 in ppR) are the same as in the underlying crystal structures because of the chosen constraints.

All theoretical methods predict that the chromophore geometries in bR and ppR are very similar, except for the extent of BLA. The geometry of the HBN differs in the X-ray, the SCC-DFTB/CHARMM, and the other theoretical structures, and the effect of these geometrical differences on excitation energies will be examined in the next section.

B. Excitation Energies and Dipole Moments of bR and ppR. Excitation energies were calculated using SORCI and OM2/MRCI on the basis of the QM/MM optimized structures (Table 2). In the following, the chromophore is treated quantum mechanically while the rest of the protein is represented by point charges as taken from the CHARMM force field.

The spectral shift between bR and ppR is 0.29 eV with SORCI and 0.30 eV with OM2/MRCI (Table 2), both values being very close to the experimental one of 0.32 eV.[14,82] The absolute energies at the SORCI level (2.34 eV for bR, 2.63 eV for ppR) are overestimated by about 0.1 eV. OM2/MRCI

Table 2. Vertical Excitation Energies ΔE_{S1-S0} (in eV)[a]

method	system	bR	ppR	ΔE_{ppR-bR}
exp[14,82]	protein	2.18	2.50	0.32
SORCI	vacuum[b,c]	1.86	1.91	0.05
	protein[b,d]	2.34	2.63	0.29
	$\Delta_{protein-vacuum}$	0.48	0.72	–
OM2/MRCI	vacuum[b,c]	2.22	2.24	0.02
	protein[b,d]	2.66	2.96	0.30
	$\Delta_{protein-vacuum}$	0.44	0.72	–
	extended HBN[b,e]	2.98	3.05	0.07
	$\Delta_{HBN-vacuum}$	0.75	0.81	–
	constrained protein[d,f]	2.66	2.99	0.33
	constrained HBN[e,f]	2.96	3.09	0.13

[a] From QM calculations on the chromophore. [b] Geometries from QM/MM optimization of the protein. [c] External point charges not included in QM calculations. [d] External point charges included in QM calculations. [e] Only point charges of Asp85/75, Asp212/201, Arg82/72, W402, W401, and W406/400 included in QM calculation. [f] Constrained geometry optimization: the chromophore was allowed to relax while the Schiff base nitrogen and the rest of the protein were fixed at the X-ray positions.

overestimates the excitation energies (2.66 eV for bR, 2.96 eV for ppR) by ~0.3 eV compared to SORCI (Table 2), but reproduces relative energies in good agreement with SORCI and the experimental results as expected from our previous study.[44]

Generally, the applied QM/MM treatment involves some approximations, in particular the neglect of environmental polarization and dispersion interactions that would redshift the excitation energy. These contributions have been addressed only by few theoretical approaches[20,75,83] and we have discussed them in some detail previously.[44] For bR and ppR, Ren et al.[20] reported dispersive red shifts of 0.15 and 0.12 eV, resulting in a very small contribution of 0.03 eV to the spectral shift.

The dipole moment may be used to assess the global electrostatic interaction between the chromophore and the protein environment. As known from experiment, the dipole moment of the chromophore changes significantly upon excitation.[84] A large change in dipole moment $|\mu_{S_1} - \mu_{S_0}|$ is indeed computed both by SORCI (10.0 D for bR, 7.9 D for ppR) and by OM2/MRCI (11.8 D for bR, 9.4 D for ppR). These values are in qualitative agreement with those reported by Hayashi et al.[21] (15.0 D for bR, 10.1 D for ppR), while in the work of Ren et al.[20] the change is smaller in bR (8.4 D) than in ppR (12.4 D).[104]

The dipole moment of the chromophore is computed to be significantly different in the protein and in a vacuum (i.e., with and without MM point charges). The corresponding differences $|\mu^{protein} - \mu^{vacuum}|$ for the S_0 ground state of bR and ppR are 6.8 and 10.1 D with SORCI, and 8.6 and 12.2 D with OM2/MRCI, respectively (the values for S_1 are similar). This shows that the ppR environment polarizes the chromophore more strongly than the bR environment.

A general discussion of the electronic structure of retinal and retinal models has already been given by various authors (see e.g., ref 44, 85, 86) and our calculations do not yield any new insights in this regard. Therefore, we refer to the Supporting Information for a Mulliken population analysis. Note that the state "S_1" labels the bright, singly excited state throughout this article, although in ppR, the dark, doubly excited state is predicted by the SORCI method to be slightly lower in energy. A similar sequence of the two states in the presence of a strong counterion has been found in CASPT2 studies of a model chromophore in rhodopsin.[87] Note that in contrast to the CASSCF/CASPT2 results in ref 88, we do not observe any mixing of the diabatic components between S_1 and S_2 or any transfer of oscillator strength to the doubly excited state.[105]

In the remainder of this section, we will investigate different factors controlling the spectral characteristics.

Role of the Chromophore Geometry. To elucidate the role of the chromophore geometry, excitation energies were calculated for the bare chromophore using either a gas-phase optimized structure or the QM/MM optimized structure of the chromophore in bR and ppR. Additionally, the nonoptimized crystal structures were used to check the effect of the minimization on the exitation energy of the bare chromophore.

For the gas-phase optimized structure of the chrompophore, we found excitation energies of 1.86 eV for SORCI and 2.16 eV for OM2/MRCI, which are similar to the values for the QM/MM optimized structures (Table 2). The latter ones deviate by less than 0.05 eV for SORCI and 0.08 eV for OM2/MRCI from those for the gas-phase optimized structures. This means that the strain exerted on the chromophore by its protein environment does not cause distortions that tune the excitation energy since the variation in the BLA is induced electrostatically and not sterically. Hence, neither SORCI (0.05 eV) nor OM2/MRCI (0.02 eV) find a significant difference between the excitation energies of the two QM/MM optimized chromophores.

For the nonoptimized chromophores taken from the crystal structures, the excitation energies (OM2: 2.23 eV for bR, 2.21 eV for ppR) agree well with those found for the QM/MM optimized structures, implying that the effect of geometry minimization is very small.

Influence of the Counterion Complex. The contribution of the counterion complex (Asp85/75, Asp212/201, and Arg82/72) to the electrostatic environment has been regarded as a key to understanding the mechanism of color tuning.[20,21,38,43] To estimate the effect of the counterion complex on the spectral shift, we calculated the excitation energies using OM2/MRCI for a model only including the point charges of the extended HBN, i.e., of the counterion complex and the three water molecules in the retinal binding pocket (extended HBN in Table 2). For these extended HBN models, we find excitation energies of 2.98 eV for bR and 3.05 for ppR (Table 2). Hence, the difference of the excitation energies decreases to 0.07 eV, i.e., the contribution of the extended HBN to the total shift is only 23%. The counterions obviously blue-shift the excitation energies strongly while the remainder of the protein causes a redshift, which is larger in bR than in ppR.

As discussed above, the HBN is less distorted in our QM/MM optimized structures than in the crystal structures. To investigate the influence of the distortion, the excitation energies

(104) However, these data are difficult to compare since in our approach and in Hayashi et al.[21] the dipole moment is calculated for the charged chromophore, while Ren et al.[20] reported the dipole moments of the complete, neutral binding pockets. Compared to OM2/MRCI and SORCI, CASSCF calculations[21] predict larger changes of the dipole moment upon excitation due to the lack of dynamical correlations.[44] For the same reason the influence of external charges on the excitation energy is overestimated with CASSCF.[44.]

(105) Whether the predicted state crossing is realistic or not, cannot be safely concluded from the current calculations, since the accuracy of SORCI and CASPT2 for the doubly excited state energy may be lower than for the singly excited one and no experimental evidence has been put forward about the first. Hence, we omit further discussion of the doubly excited state.

were recalculated using the crystal structures optimized under constraints: only the chromophore geometry was allowed to relax, whereas the position of the Schiff base nitrogen and the rest of the protein were fixed, thus preserving the distorted structure of the HBN. The excitation energies were computed incorporating either the whole protein or only the extended HBN as point charges (last two lines in Table 2).

For the whole protein, the spectral shift between bR and ppR increases by 0.03 eV to 0.33 eV, indicating that the slight differences in the counterion residue geometry and the distorted HBN have only little impact on the spectral shift. The difference in excitation energies for the extended HBN models increases from 0.07 eV as evaluated with the QM/MM optimized structures to 0.13 eV (Table 2). This shows that the distortion of the HBN structure has some influence on the excitation energy, which may be underestimated in our QM/MM model. Nonetheless, it confirms that the overall contribution of the counterion residues and the HBN to the spectral shift (about 30−40%, or 0.1 eV) is much smaller than previously assumed.

In particular, preceding theoretical studies proposed structural differences in the (extended) HBN to cause the complete spectral shift,[20,21] e.g., the increased distance between the Schiff base nitrogen and Asp212 in bR relative to ppR (Hayashi et al.[21]). We investigated this aspect in detail as well. Results of this analysis can be found in the Supporting Information. We find that this aspect contributes to the spectral shift, however, not to the extent as reported in the previous studies.

C. Perturbation Analysis. To analyze the influence of the individual amino acids, each residue was successively replaced by glycine and the excitation energy was recalculated using OM2/MRCI without further minimization of the protein. All amino acids having a notable influence (larger than 0.005 eV) on the excitation energy are discussed below. These amino acids can be grouped into four categories, (i) the counterion residues Asp85/75, Asp212/201, and the nearby Arg82/72, (ii) other charged residues located at the extracellular side of the protein, (iii) conserved residues in the binding pocket, and (iv) remaining neutral, nonconserved residues. The influence of the water molecules in the extended HBN was determined by simply setting the respective charges to zero. The results of this perturbation analysis are summarized in Table 3.

Influence of the Counterion Residues and the Extended HBN. The counterion residues Asp85/75 and Asp212/201 (in bR/ppR) cause large blue shifts of 0.3−0.4 eV. The effect of Arg82/72 is small and opposite in bR (−0.01 eV) and ppR (0.02 eV). The guanidinium group of Arg82/72 has a different orientation in the two proteins. It is oriented toward the chromophore in bR, forming a hydrogen bond with the extended HBN, whereas it is pointing toward the extracellular side in ppR, forming a salt bridge with Asp193. The different orientation may cause Arg82/72 to affect the excitation energy in opposite direction. This is in qualitative agreement with the findings of Ren et al.;[20] however, since their calculations predict a much more pronounced effect, they proposed Arg82/72 to be responsible for the complete spectral shift.

The water molecules in the HBN seem to be of minor importance for the spectral difference between bR and ppR (Table 3).

The replacement of all three charged residues (Asp85/75, Asp212/201, and Arg82/72) plus the water molecules in their proximity causes a strong red shift of −0.66 eV for bR and −0.73 eV for ppR, i.e., omitting the HBN reduces the spectral shift between bR and ppR from 0.30 to 0.23 eV. The complete extended HBN contributes therefore 0.07 eV to the total spectral shift. This is consistent with the results in sec. IIIB and confirms that the counterion residues account only for part of the spectral shift.

Table 3. Calculated OM2/MRCI Shifts of the Vertical Excitation Energies $\Delta\Delta E_{\text{mutant}-\text{wildtype}}$ (in eV) and Position for Glycine-Mutants of Selected Residues[a]

bR/ppR	bR	ppR	$\Delta E_{\text{ppR}-\text{bR}}$	position	bp
counterion residues					
Asp85/75	−0.39	−0.39	0.00	H−C	+
Asp212/201	−0.37	−0.32	0.05	H−G	+
Arg82/72	0.01	−0.02	−0.03	H−C	+
water molecules in the HBN[b]					
W401/W401	0.02	0.02	0.00	−	+
W402/W402	−0.09	−0.08	−0.01	−	+
W406/W400	0.03	0.02	0.01	−	+
remaining charged residues					
Glu194/Pro183	0.08	0.00	−0.08	H−F	−
GluH204/Asp193	0.01	0.04	0.03	H−G	−
conserved residues					
Trp182/171	−0.01(8)	−0.01(4)	0.00	H−F	+
Tyr185/174	−0.02(5)	−0.01(2)	0.01	H−F	+
Trp189/178	0.02	0.01	−0.01	H−F	+
Tyr57/51	0.02	0.02	0.00	H−B	−
Tyr83/73	0.01(8)	0.00(4)	−0.01	H−C	+
Trp86/76	0.03	0.03	0.00	H−C	+
Thr89/79	−0.03	−0.03	0.00	H−C	+
Thr90/80	0.04	0.03	−0.01	H−C	+

[a] The QM-region in OM2/MRCI consists of the chromophore. The position column indicates the location of the mutated residue, i.e., H−C indicates this residue to be located at helix C (etc.); the bp column specifies whether the residue is located in the binding pocket. [b] The partial charges of the water molecules were deleted for the calculation of the shift.

Note that the effects of the counterion residues and water molecules in Table 3 are not additive. Therefore, the sum of the individual effects differs from the results obtained through replacement of the complete extended HBN.

Influence of Other Charged Residues. The effect of all solvent exposed amino acids on the excitation energies is, in accordance with experimental results,[89] small since their charges are reduced due to the solvent screening modeled by the charge scaling procedure.

Among the remaining charged residues, only the anions Glu194 in bR and Asp193 in ppR have a sizable influence (Table 3). Both residues red-shift the excitation energy, by 0.08 eV (Glu194 in bR) and 0.04 eV (Asp193 in ppR), respectively. They belong to a large HBN at the extracellular side of the protein that connects the Schiff base region with Glu194 and Glu204 in bR and with Asp193 in ppR (via several water molecules and Arg82/72).

The simultaneous replacement of the extended HBN and the charged groups Glu194/Asp193 leads to a red shift of −0.59 eV in bR and of −0.68 eV in ppR. Therefore, omitting the complex network of hydrogen bonded and charged residues at the extracellular side of bR and ppR reduces the spectral shift between bR and ppR by about 0.09 eV to a value of 0.21 eV. This is only slightly less than the value obtained for the extended HBN alone (0.23 eV, see above).

Influence of Conserved Residues in the Binding Pocket. The conserved aromatic tyrosines and tryptophanes have only

Table 4. Calculated OM2/MRCI Shifts of the Vertical Excitation Energies $\Delta\Delta E_{mutant-wildtype}$ (in eV) and Position for Glycine-Mutants of Polar Residues[a]

bR/ppR	bR	ppR	ΔE_{ppR-bR}	position	bp	exp.
Trp138/Phe127	0.01	0.00	−0.01	H−E	+	+
Ser141/Gly130	0.07		−0.07	H−E	+	+
Thr142/Ala131	0.03	0.00	−0.03	H−E	+	+
Met145/Phe134	0.02	0.01	−0.01	H−E	+	+
Ile119/Met109	0.00	0.01	0.01	H−D	+	+
Ala215/Thr204	0.00	−0.07	−0.07	H−G	+	+
Met118/Val108	0.00(4)	−0.00(1)	−0.01	H−D	+	+
Thr121/Ala111	0.02	0.00	−0.02	H−D	−	−
Ser214/Val203	0.01	0.00	−0.01	H−G	−	−
Pro50/Ser44	0.00	0.01	0.01	H−B	−	−
Ser183/Ala172	0.01	0.00	−0.01	H−F	−	−
Thr55/Val49	0.00	0.00	0.00	H−B	−	−
Gly116/Thr106		−0.01	−0.01	H−D	−	−
all	0.16	−0.04	−0.20		−	−

[a] The QM-region in OM2/MRCI consists of the chromophore. The position column indicates the location of the mutated residue, i.e., H−C indicates this residue to be located at helix C (etc.); the bp column specifies whether the respective residue is located in the binding pocket.

a minor influence on the excitation energy and the spectral shift (Table 3). Similar results were found by Ren et al.[20] for Trp86/76, Trp182/171, and Tyr185/174. The two conserved threonines (Thr89/79, Thr90/80) do not influence the spectral shift either, as their effect is the same in bR and ppR.

Replacing all residues of this group simultaneously leads to blue shifts of 0.07 eV for bR and 0.05 eV for ppR, and hence to a differential shift of 0.02 eV. It should be noted again, however, that our calculations neglect the effects of protein polarization and dispersion, which were estimated[20] to cause an additional differential red shift of 0.03 eV (see sec. III B).

Influence of Polar Residues in the Binding Pocket. This group consists of all residues that have a sizable influence on the excitation energy and are neither charged nor conserved residues. Several of these residues (see last column in Table 4) have also been analyzed in experimental mutation studies,[16,19] which will be discussed in detail in sec. III D.

Among the residues of this group, only the replacements Ala215/Thr204, Ser141/Gly130, and Thr142/Ala131 lead to a substantial differential shift (Table 4). The replacements Thr121/Ala111, Pro50/Ser44, and Ser214/Val203 cause minor but noticeable differential shifts, even though they are further away from the chromophore and do not belong to the binding pocket. For the remaining substitutions, the differential shift is less than 0.01 eV.

The simultaneous replacement of all polar residues (Table 4) leads to a blue shift of 0.16 eV in bR and a red shift of −0.04 eV in ppR. Thus, these residues contribute 0.20 eV to the overall spectral shift of 0.30 eV. A summation of all individual contributions yields the same value (0.20 eV), indicating that cooperative effects play a minor role in this case.

D. Mutation Experiments in ppR. Several mutation studies, in particular those of Shimono and co-workers,[15−19] have addressed the role of various amino acids in the spectral tuning between bR and ppR. To compare our results directly to these experiments, we mutated individual residues or groups of residues in ppR to their counterparts in bR. After geometry optimization of either the mutated residue(s) or the whole protein, the excitation energies were recalculated using OM2/MRCI (Table 5). Those of the most important mutations were also determined at the SORCI level.

Table 5. Calculated Shifts of the Vertical Excitation Energies $\Delta\Delta E_{mutant-wildtype}$ (in eV) of Various ppR Mutants[a] Calculated with OM2/MRCI and SORCI[b]

		OM2/MRCI		SORCI	
	exp.[16,19]	local relaxation[c]	full relaxation	local relaxation[c]	full relaxation
Val108Met	−0.015	0.01	−0.02	0.00	−0.05
Gly130Ser	−0.02	−0.03	−0.06	−0.01	0.00
Thr204Ala	−0.044	−0.07	−0.06	−0.05	−0.05
Gly130Ser/ Thr204Ala	−0.073	−0.11	−0.13	−0.07	−0.07
Val108Met/ Gly130Ser	−0.049	−0.02	−0.07	−0.01	−0.06
Val108Met/ Thr204Ala	−0.049	−0.06	−0.08	−0.04	−0.09
Val108Met/ Gly130Ser/ Thr204Ala	−0.077	−0.09	−0.14	−0.05	−0.11
Ile43Val	−0.015	0.00	−0.01		
Ile83Leu	−0.01	0.00	0.00		
Asn105AspH	0.00	−0.00	0.01		
Met109Ile	0.01	0.02	0.03		
Ala131Thr	−0.015	−0.01	−0.01		
Phe127Trp	0.005	−0.00	0.01		
Phe134Met	−0.005	−0.01	0.00		
bR/ppR	−0.118	−0.13	−0.19	−0.07	−0.16

[a] The nomenclature was adopted from[16,19] the first residue label and the residue number refer to ppR, and the second residue label specifies the corresponding amino acid of bR (ppR → bR). [b] The QM-region consists of the chromophore. [c]Reminimization of the mutated residue only.

The results show (Table 5) that complete optimization of the protein after mutation yields larger shifts than optimization of the mutated residue(s) only. The agreement with the experimental shifts, even for the examined double, triple and multiple mutants, is fairly good using SORCI and the full relaxation scheme (ii), while the OM2/MRCI shifts are generally somewhat overestimated.

In the following, we will focus on the OM2/MRCI values to facilitate comparisons with the preceding OM2/MRCI-based perturbation analysis (sec. IIIC).

Among the single mutations, Thr204Ala, Gly130Ser, Val108Met, Ala131Thr, and Ile43Val[106] lead to large effects. The largest impact is produced experimentally as well as theoretically by the mutations Thr204Ala (−0.06 eV; exp. −0.04 eV) and Gly130Ser (−0.06 eV; exp. −0.02 eV), whereas the other replacements (Val108Met, Ala131Thr, Ile43Val) are less effective, each with an experimentally measured shift of −0.015 eV (120 cm^{-1}).

In general, the absolute and relative contributions of these residues to the spectral shift have been predicted quite well by the perturbation analysis (Table 4), which gives significant contributions for the replacements Thr204Ala, Gly130Ser, and Ala131Thr (−0.07, −0.07, and −0.03 eV), and a minor one for Val108Met (−0.005 eV), which is underestimated but has the correct sign. The substitution Ile43Val does not contribute in the perturbation analysis because both residues are unpolar (and because the perturbation analysis does not include relaxation of the geometry).

The remaining five (Ile83Leu, Asn105AspH, Met109Ile, Phe127Trp, Phe134Met) mutations do not show any significant shift, neither in the experiment nor in our calculations, which is also in accord with the results from the perturbation analysis (sec. IIIC).

Table 6. Calculated Shifts of the N−H Stretch Vibration and Bond Length Alternation for bR, ppR and the bR/ppR Mutant

	ν(NH) − ν_{bR}(NH) [cm^{-1}]	BLA [Å]	$\Delta E_{S_1-S_0}$ [eV]
bR		0.056	2.66
bR/ppR	−29	0.059	2.77
ppR	−25	0.065	2.96

In addition to the single replacements, double, triple, and multiple mutants were also investigated. Of special importance is the triple mutant Val108Met/Gly130Ser/Thr204Ala, whose three sites are conserved among the long-wavelength rhodopsins hR, bR and sRI, but not in ppR, and are therefore expected to be involved in the spectral tuning of archaeal rhodopsins. However, the calculated shift (OM2/MRCI −0.14 eV, SORCI −0.11 eV) as well as the experimentally observed shift (−0.08 eV) is only a fraction of the complete shift between bR and ppR (exp. ∼30%).

A second important mutant is the multiple mutant bR/ppR, in which all 10 different residues of the binding pocket within 5 Å are substituted such that the binding pocket of this mutant is identical to that of bR. Even so, the mutant has a spectral shift of only −0.12 eV (∼40%) experimentally. Our calculations predict −0.19 eV (∼60%) for OM2/MRCI and −0.16 eV (∼50%) for SORCI. Thus, the calculations reproduce but overestimate the effect. The computed OM2/MRCI shift agrees nicely with the value obtained in the perturbation analysis (Table 4) when the side chains of all polar residues of the binding pocket are removed simultaneously (−0.20 eV).

Furthermore, the results are consistent with a study[18] in which the helices D, E, and G were identified as the determining factors for color regulation accounting for around 80% of the spectral shift. Almost all residues with sizable impact on the excitation energies (Table 4) found in the present study are located on these helices.

E. Vibrational Analysis. Vibrational properties of rhodopsins have been widely used to elucidate various issues in bR and ppR, e.g., structures and structural changes, the mechanism of proton transport in bR and, in particular, the mechanism of the spectral tuning.[38,43,81,90] In this work, two aspects of the vibrational characteristics of the chromophore backbone and of the Schiff base were studied for bR, ppR, and the bR/ppR mutant.

The NH stretching mode of the Schiff base is of particular interest because it reflects the strength of the hydrogen bond of the Schiff base. By performing QM/MM molecular dynamics simulations, we calculated the N−H stretching frequency in bR, ppR and the bR/ppR mutant via the velocity autocorrelation function.

In going from bR to ppR, we find this frequency shifted to lower wavenumbers by 25 cm^{-1} (Table 6), indicating a stronger hydrogen bond of the Schiff base to W402 in ppR. The calculated shift compares well to the experimentally observed one of 32−33 cm^{-1} [43] for the N−D stretching vibration of the deuterated Schiff base. For the bR/ppR mutant, we find a similar frequency ($\Delta\nu$ = 4 cm^{-1}) as for ppR (Table 6), implying a similar hydrogen bond strength. This agrees well with experimental results[17] which demonstrate that the Schiff base vibrations remain ppR-like while the chromophore bands are altered from ppR-like to bR-like.

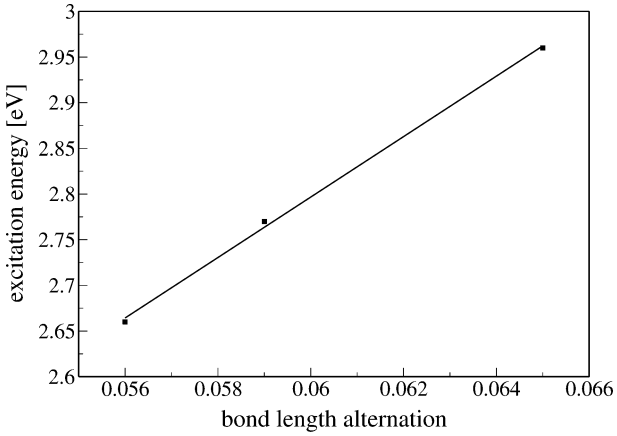

Figure 2. Correlation of bond length alternation and excitation energy for bR, ppR, and the bR/ppR mutant.

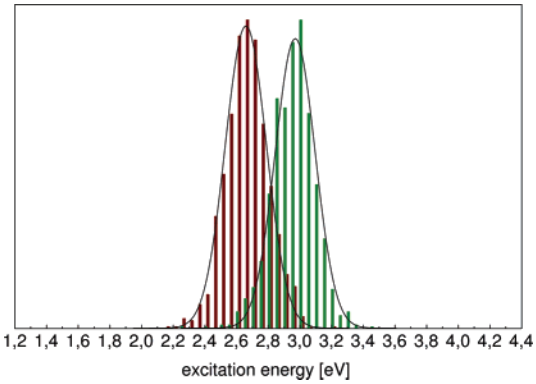

Figure 3. Calculated histograms for the excitation energy of the S_0-S_1 transition for bR (red) and ppR (green).

The vibrations of the chromophore backbone, in particular the C═C stretching modes, are a sensitive probe for the electrostatic interaction of the retinal with the protein environment, especially for the potential gradient along the polyene chain.[28,91−93] It is well-known that the C═C stretching frequency correlates with the bond length alternation (BLA),[28,91,94] which increases from bR (0.056 Å) via the bR/ppR mutant (0.059 Å) to ppR (0.065 Å). A similar increase is seen in the calculated excitation energies (Table 6). We find a linear relationship between the BLA and the excitation energies (Figure 2), which is consistent with the experimentally characterized linear relationship between C═C stretching frequencies and the absorption maximum.[28] These results indicate that the electrostatic interaction with the protein environment is very similar in the bR/ppR mutant and in bR, which share the same binding pocket.

F. Dynamics. To investigate the effects of structural fluctuations at room temperature on various properties of the systems, in particular on the stability of the HBN, QM/MM molecular dynamics simulations were performed for both proteins. As an approximation to the absorption spectra, histograms of the excitation energy (Figure 3) along the trajectories[75] were calculated. A more profound line shape analysis would be preferable but is beyond the scope of the present study.

Absorption maxima λ_{max} of 2.65 and 2.97 eV were found for bR and ppR, respectively, using Gaussian fits, thus reproducing the spectral shift between bR and ppR (0.32 eV; exp. 0.32 eV). The calculated line width of 2097 cm^{-1} (0.26

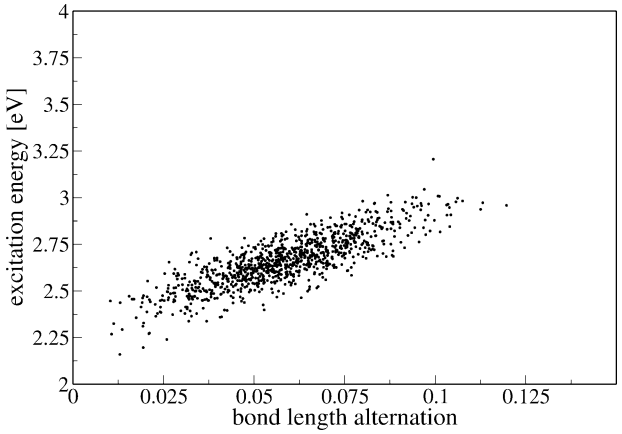

Figure 4. Correlation of bond length alternation and excitation energy for bR.

eV) for bR is comparable to the experimental one of 2860 cm^{-1}.[95]

For the geometrical parameters of the extended HBN, we find fluctuations of about 0.2 Å around the equilibrium values (see Supporting Information) thus indicating a fairly rigid structure of the HBN. This stability of the HBN and of its interaction with the chromophore and counterion complex is a necessary requirement for applying a static approach that draws conclusions from the properties of optimized QM/MM structures.

The dynamics runs allow us to analyze the influence of structural fluctuations of the protein[96] on the excitation energy, by calculating the correlation coefficients between various geometrical parameters and the excitation energy along the MD trajectories. The results show a strong correlation (0.83) between the BLA and the excitation energy (Figure 4), again consistent with the linear relationship between the excitation energy and the C═C stretching vibration of the chromophore[28] (Figure 2) described in the preceding section.

The correlation of the excitation energy with individual distances between the Schiff base and the counterion residues (e.g., $N_\zeta - C_\gamma$) is unexpectedly small (less than 0.1). The electrostatic potential generated by the partial charges on the counterion residues at the position of the Schiff-base nitrogen provides a collective coordinate that takes into account the correlated fluctuation of the counterion residues, which are not described using only single decoupled distance measures. A noticeable correlation (−0.3) is found between this potential and the excitation energy. Thus, the (collective) distance of the counterions from the chromophore influences the excitation energies, but this correlation is considerably weaker than that for the BLA.

IV. Discussion

Several experimental[16,18,19] and theoretical investigations[20,21] have addressed the spectral shift between bR and ppR, examining the different mechanisms of color tuning (i)−(iii) outlined in the Introduction. Our calculations allow for a distinction between these factors and a quantitative evaluation of their individual contribution.

(i) The differences between the chromophore structures of bR and ppR are already small in the crystal structures and nearly removed by the present QM/MM geometry optimizations, in agreement with previous theoretical studies.[21,20] The remaining difference concerns essentially only the BLA and gives rise to a difference in excitation energies of 0.05 eV at the SORCI level of theory and 0.02 eV with OM2/MRCI, which is only a small contribution to the shift of the absorption maximum.[107] Even when using the nonoptimized X-ray structures, the difference in the OM2/MRCI excitation energies is not larger.

(ii) The polar and charged groups of the protein environment in bR and ppR interact differently with the charge density distribution on the chromophore in its ground and excited state, thereby stabilizing or destabilizing the respective state and so modulating the excitation energy. This polarization of the chromophore is reflected in the bond length alternation along the polyene chain[108] as well as in the change of the dipole moment (with respect to vacuum). Both effects are seen in the present study. The larger bond length alternation in ppR as well as the larger change of the dipole moment due to the protein interaction ($|\mu_{S_0}^{protein} - \mu_{S_0}^{vacuum}|$) indicate a stronger electrostatic interaction with the protein in ppR compared to bR.

Furthermore, the vibrations of the chromophore backbone, in particular the C═C stretching modes, probe the electrostatic interaction of the polarized chromophore with the protein environment very sensitively.[28,91−93] Using the bond length alternation as a measure for the C═C stretching frequencies,[28] our calculations for bR, ppR and the bR/ppR mutant (a multiple mutant in which the 10 different amino acids of the binding pocket of ppR are mutated to their corresponding residues in bR) reproduce an experimentally observed linear correlation between the C═C stretching frequencies and the absorption maximum[28,33,97] very well. The comparison of bR, ppR and the bR/ppR mutant demonstrates clearly that the chromophore vibrations in bR/ppR are bR-like, in agreement with experiment.[17] This points to a very similar electrostatic interaction of the chromophore with the protein in bR and this mutant, which means that this interaction is dominated by the binding pocket.

In addition to these global aspects, the results of the perturbation analysis and mutation experiments provide a detailed picture of the interaction of individual polar and charged groups of the environment with the chromophore. In agreement with experimental data, several sites (e.g., Thr204Ala, Gly130Ser, Val108Met, Ala131Thr) located in the binding pocket have a significant impact, however, none of them is solely responsible for the complete shift. Moreover, the perturbation analysis reveals a small but distinct influence of some sites (e.g., Ala111Thr, Ser44Pro) which do not belong to the binding pocket and have not been experimentally studied yet.

Nevertheless, the interactions with polar and charged groups account only for a fraction, albeit a major fraction, of the observed spectral shift. The analysis of multiple mutants emphasizes this fact. The bR/ppR mutant[16] shows experimentally only 44% of the spectral shift; our calculations yield ∼50%, in good agreement with experiment. These results confirm that none of the residues in the binding pocket is solely responsible for the spectral shift.

(iii) The interaction of the counterion residues with the chromophore strongly depends on their distance[33,34] from the

(106) The nomenclature was adopted from[16,19] and corresponds to the mutation ppR → bR. The residue numbers refer to ppR.
(107) Using the chromophore structures obtained by QM/MM optimization of the whole protein, a distinction between distortions induced by steric confinement and effects induced by electrostatic interactions with the protein is not possible.
(108) It has been shown that the bond length alternation of the chromophore increases in the presence of a counterion close to the Schiff base.[44,98]

Schiff base but also on other charged and polar groups that are connected to the HBN.

Therefore, this often discussed mechanism of color tuning focuses on the structure of the counterion complex and the three water molecules connecting the Schiff base and the counterion residues (i.e., the extended HBN). The structural differences between bR and ppR mainly concern the different orientation of the guanidinium group of Arg82/72 and a distortion of the pentagonal cluster formed by the two aspartic acids of the counterion complex and the three water molecules[81] in ppR.

We have estimated the contribution of the extended HBN to the spectral shift between bR and ppR by including only the residues of the extended HBN as point charges in the excited-state calculations, excluding the remainder of the protein. For this extended HBN model, a contribution of 23% to the spectral shift is found. This value agrees well with the results of the perturbation analysis.

Including further residues from the extracellular site (Glu204 for bR, Asp193 for ppR) in the perturbation analysis yields a contribution of the complete hydrogen bonded network at the extracellular side of ~30% to the spectral shift.

This value seems to be a lower bound because our QM/MM minimized structures do not distort the pentagonal cluster in ppR to the extent that is found experimentally. When calculating the excitation energy with partially optimized structures (constrained to conserve the HBN positions from the crystal structure), we obtain a contribution of 40% to the spectral shift for the counterion complex, instead of 23% with our fully optimized structures. Therefore, considering the distortion of the HBN and further residues from the extracellular site, the contribution of the counterion complex to the spectral shift may be as high as 40%.

The interaction of the counterion complex with the chromophore also affects the vibrations of the Schiff base. For instance, the NH stretching mode of the Schiff base reflects the strength of the hydrogen bond of the Schiff base to the counterion complex. Our calculations yield a clearly increased frequency for bR compared to ppR whereas it is essentially unchanged (even lower) in the bR/ppR mutant. This suggests, in agreement with the experiment, a stronger hydrogen bond of the Schiff base with the counterion complex in ppR which is hardly influenced by the mutations in the binding pocket that are present in the bR/ppR mutant.

The stronger hydrogen bond in ppR was supposed to originate from small changes in the HBN and related to the spectral blue shift in ppR.[17,38] Results from X-ray crystallography[35,36] and the analysis of the O−D stretching vibrations of the water molecules in the HBN[43,81] support a distorted HBN structure in ppR.

In summary, our results indicate that the interaction with the extended HBN and with the binding pocket equally contribute to the spectral shift. Taking into account the effect of the distorted HBN, the influence of the extended counterion region (including Glu204 for bR and Asp193 for ppR) is estimated to cause about ~40% of the spectral shift. Our best estimate for the contribution of the binding pocket amounts to about 40−50%.

These results explain why the experimental absorption maximum of the bR/ppR mutant is less shifted toward the bR value than expected.[16] Due to the mutations, the binding pocket of this mutant is bR-like, whereas the counterion region remains ppR-like. Thus, the replacement of the amino acids within 5 Å of the chromophore is not sufficient to transform ppR into bR with regard to electronic excitation.

V. Conclusion

The good agreement between our theoretical and the experimental results shows that modern quantum mechanical methods can not only reproduce but also interpret spectral properties of photoproteins. Our approach of combining very efficient (SCC-DFTB, OM2/MRCI) and very accurate (SORCI) methods allows a comprehensive, qualitative investigation of the spectral shift including the analysis of dynamical effects.

Both the calculated shift of the absorption maximum λ_{max} of ppR relative to bR and the magnitude of the bandwidth agree well with experimental results. Mutation studies and the analysis of vibrational properties have provided further insight into the contribution of different factors to the spectral shift.

We have shown that our methodology correctly describes even the subtle effects of point and multiple mutations. So we reproduced the properties of bR, ppR, and the bR/ppR mutant in the Schiff base region, illustrated by the N−H stretching vibration, as well as in the binding pocket, exemplified, e.g., by the experimentally observed linear correlation between the C═C stretching frequencies of the chromophore and the absorption maximum[28,33,93].

Numerous sources contribute to the spectral shift between bR and ppR. The two main and equally important factors, which are responsible for about 90% of the total shift, are the different neutral amino acids in the binding pocket and the difference in the extended hydrogen bonded network at the extracellular side of the proteins. The rest may be accounted for by geometrical differences between the chromophores and the conserved, polarizable residues, i.e., by slight differences in their electrostatic interaction, including protein polarization and differential dispersive interactions.

Acknowledgment. The authors acknowledge valuable discussions with Edda Kloppmann, Matthias Ullmann and Volker Buβ. This work was supported by the Deutsche Forschungsgemeinschaft through Forschergruppe 490 (M.E.) and SFB 663 (W.T.). Some of the computations were carried out at the regional computing center in Cologne (RRZK) and on the joint cluster PLING of theoretical physics and Paderborn center for parallel computing (PC^2). M.H. thanks T. Niehaus for his help concerning the vibrational analysis. K.S. and E.T. acknowledge support by NIH grant P41-RR05969, NSF Grant No. MCB02-34938 and supercomputer time provided by Pittsburgh Supercomputer Center and the National Center for Supercomputing Applications via National Resources Allocation Committee grant MCA93S028.

Supporting Information Available: Dipole moments and Mulliken charges for QM/MM minimized structures, geometrical data for QM/MM molecular dynamic simulations and additional analysis for excitation energies. This material is available free of charge via the Internet at http://pubs.acs.org.

JA062082I